Section 3

Computational studies including new techniques, the effect of varying model resolution, parallel processing

CONFORMAL OVERSET GRIDS

R. James Purser and Miodrag Rančić[1],
IMSG at NOAA/NCEP/EMC, Camp Springs, Maryland, USA.

email: jim.purser@noaa.gov   miodrag.rancic@noaa.gov

The well-known inefficiencies and numerical problems in numerical weather prediction associated with the convergence of meridians and the polar singularies of a latitude-longitude-based grid system have spurred the development of polyhedron-based alternative grids, such the cubed sphere and the (triangular-gridded) icosahedron. Moreover, except at the vertices, the continuous mappings for these configurations can be made perfectly conformal (angle preserving), which substantially simplifies the adaptation of existing grid-based regional models to these global geometries. However, the unavoidable vertex singularities on *continuous* polyhedral grids still remain too strong to avoid severe numerical difficulties for any model based on spatial finite differencing. "Oversetting" is a remedy that preserves smooth grid
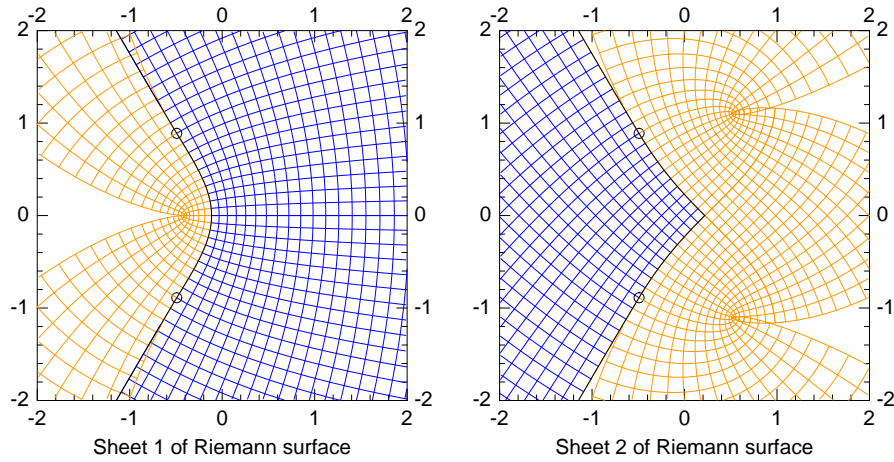

Figure 1: Detail of junction of three square map panels of the physical solution domain (blue grids) and their extrapolation (orange) that enable oversets for consistent blending of model solutions each time step. The strong mapping singularities are expelled from the physical portion of the grid, leaving only the very weak 'branch point' singularities (indicated as small circles) at the edges separating one map panels from its paired neighbors

---

[1]With support from National Science Foundation grant ATM-0739518.

continuity across the middle sections of each edge of the original generating polyhedron, but which relinquishes continuity in the vicinity of each vertex in favor of artificially grafted smooth replacements and extensions of the grid there to provide a region of self-overlapping that is free of strong map singularies. Oversetting requires instead a frequent interpolation and merging of the locally duplicated solutions. A purely localized disfigurement of the grid in this way, however carefully smoothed and blended, cannot preserve the desirable property of conformality.

We have developed new techniques that do enable a globally consistent and perfectly conformal polyhedral mapping to be constructed with the oversets automatically supplied in the regions where there would otherwise be vertex singularities (Fig. 1). The methods are based on the construction of complex analytic functions that involve Riemann surfaces where the inverse mapping (sphere to polyhedron) is at least two-valued. Moreover, the technique is capable of an immediate and potentially valuable extension (e.g., Fig. 2) to smooth mappings no longer constrained to correspond to *convex* polyhedra, and which enables the resolution of the generated grid to possess multiple regions of locally enhanced resolution. Such configurations suggest more unified alternatives to the traditional separation of models for global, regional and various further nested tasks of operational models.
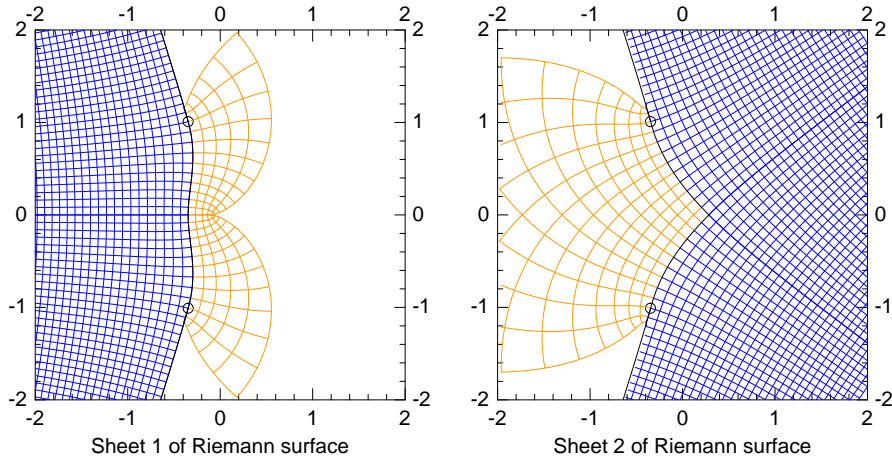

Figure 2: The Riemann surface solution showing a junction of map panels (blue grids) and their extrapolation (orange) to a region from which consistent oversets of the grid can be created. This case, with five square map panels meeting, no longer corresponds to any convex polyhedron, but configurations of this kind can be exploited to provide enhanced resolution at selected geographical locations of a single unified global grid.

Development of a nonhydrostatic global spectral atmospheric model using double Fourier series

Hiromasa Yoshimura
Meteorological Research Institute, Japan Meteorological Agency
E-mail: hyoshimu@mri-jma.go.jp

1. Introduction

The Global Spectral Atmospheric Model (GSAM) of the Japan Meteorological Agency (JMA) is a hydrostatic spectral model using spherical harmonics. In GSAM, a two-time-level semi-implicit scheme and a vertically conservative semi-Lagrangian scheme (Yoshimura and Matsumura 2005; Yukimoto et al. 2011) are used to allow a longer timestep, and the reduced grid (Miyamoto 2006, 2009) is used to save computational cost. We have developed a nonhydrostatic version of GSAM for higher resolutions. We have also developed an option of using double Fourier series instead of spherical harmonics as spectral basis functions for efficiency.

2. Development of nonhydrostatic spectral model

We have developed a nonhydrostatic dynamical core for GSAM. We use the following prognostic equations:

$$\pi \equiv A(\eta) + B(\eta)\pi_s \tag{1}$$

$$P \equiv \frac{p - \pi}{\pi} \tag{2}$$

$$\frac{d(\mathbf{v} + 2\mathbf{\Omega} \times \mathbf{r})}{dt} = -RT\left(\frac{1}{\pi}\nabla\pi + \frac{1}{1+P}\nabla P\right) - \nabla\Phi - \nabla\Phi\,\underline{\frac{1}{\partial\pi/\partial\eta}\frac{\partial(\pi P)}{\partial\eta}} \tag{3}$$

$$\frac{dw}{dt} = g\frac{1}{\partial\pi/\partial\eta}\frac{\partial(\pi P)}{\partial\eta} \tag{4}$$

$$\frac{dT}{dt} = -\frac{RT}{c_v}D_3 \tag{5}$$

$$\frac{\partial}{\partial t}\left(\frac{\partial\pi}{\partial\eta}\right) + \nabla\cdot\left(\mathbf{v}\frac{\partial\pi}{\partial\eta}\right) + \frac{\partial}{\partial\eta}\left(\dot{\eta}\frac{\partial\pi}{\partial\eta}\right) = 0 \tag{6}$$

$$\frac{1}{1+P}\frac{dP}{dt} = -\frac{1}{\pi}\frac{d\pi}{dt} - \frac{c_p}{c_v}D_3 \tag{7}$$

$$D_3 \equiv \nabla\cdot\mathbf{v} + \frac{\pi(1+P)}{RT}\nabla\Phi\cdot\left(\underline{\frac{1}{\partial\pi/\partial\eta}\frac{\partial\mathbf{v}}{\partial\eta}}\right) - \frac{\pi(1+P)}{RT}\frac{g}{\partial\pi/\partial\eta}\frac{\partial w}{\partial\eta} \tag{8}$$

$$\frac{\partial\Phi}{\partial\eta} = -\frac{RT}{1+P}\frac{1}{\pi}\frac{\partial\pi}{\partial\eta} \tag{9}$$

where, p is pressure, π is hydrostatic pressure, π_s is surface hydrostatic pressure, η is a hybrid vertical coordinate of $\sigma(=\pi/\pi_s)$ and p, t is time, $\mathbf{v}$ is the horizontal wind vector, w is vertical wind, T is temperature, D_3 is 3-dimensional divergence of the wind, Φ is geopotential height, $\mathbf{\Omega}$ is the earth's rotation, $\mathbf{r}$ is the radial position vector, R is gas constant, c_p is specific heat capacity at constant pressure, and c_v is specific heat capacity at constant volume. These equations are substantially the same as those of the ALADIN-NH nonhydrostatic limited-area spectral model (Bubnová et al. 1995; Bénard et al. 2010) and those of the nonhydrostatic version of IFS (Wedi and Smolarkiewicz 2009). But there are some differences in the way of integration. In Bénard et al. (2010), an iterative centered implicit (ICI) scheme, in which whole terms are treated implicitly through iteration, is used to enhance stability. In our nonhydrostatic model, a non-constant coefficient semi-implicit scheme is used, in which linear terms are treated implicitly and residual nonlinear terms are treated explicitly. The coefficients of some of the linear terms are set to be non-constant in time and space. When linearizing the underlined terms in Eqs. (3) and (8), which relate to sound waves, the present values of $\nabla\Phi\cdot\partial\eta/\partial\pi$ and $\pi/RT\cdot\nabla\Phi\cdot\partial\eta/\partial\pi$ are used as non-constant coefficients. These values become large where the orography is steep. Using not only constant coefficients but also non-constant ones contributes to enhance stability because the approximation by the linear terms becomes better and the residual nonlinear terms become smaller. A preconditioned generalized conjugate residual (GCR) method, a fast-convergent iteration method, is used to solve simultaneous linear equations along with the non-constant coefficient semi-implicit scheme, where a constant coefficient semi-implicit calculation is used as a preconditioner. At the 15km or coarser horizontal resolutions, only one iteration is enough to converge in our test runs. The non-constant coefficient semi-implicit scheme with the preconditioned GCR method is more efficient compared with ICI, because only the two linearized terms underlined are needed to be recalculated per iteration in grid-space.

3. Development of double Fourier series option

We have succeeded in developing not only a hydrostatic double Fourier series model (Yoshimura and

Matsumura 2005) but also a nonhydrostatic one. In a double Fourier series model, the fast Fourier transform is used instead of the Legendre transform, which reduces computational cost in high resolutions. We use the same type of double Fourier series as in the Eulerian global shallow water model in Cheong (2000). The coefficient of the 4th-order diffusion term (i.e. biharmonic spectral filter in Cheong 2002) in the double Fourier series GSAM is as large as in the spherical harmonics GSAM and not needed to be larger. Strong spectral filters (e.g. spherical harmonics filter) are not necessary in our semi-implicit semi-Lagrangian double Fourier series model.

4. Test runs

Two-day test runs of the hydrostatic GSAM and the nonhydrostatic version of GSAM are performed from the initial conditions on 24 June 2011 at the TL1279L60 (15km horizontal grid) resolution. Figure 1 shows the 2-day mean convective and large-scale condensation precipitation of the hydrostatic and the nonhydrostatic models. The difference of precipitation between the hydrostatic and nonhydrostatic models is small. But in some mountain regions, large-scale condensation precipitation is apparently larger in the hydrostatic model than in the nonhydrostatic model. Here, only the results of the models using double Fourier series are shown. The results of the spherical harmonics and the double Fourier series models are very close. In this resolution, computational time in the double Fourier series model is about 0.7~0.8 times as long as that in the spherical harmonics model.
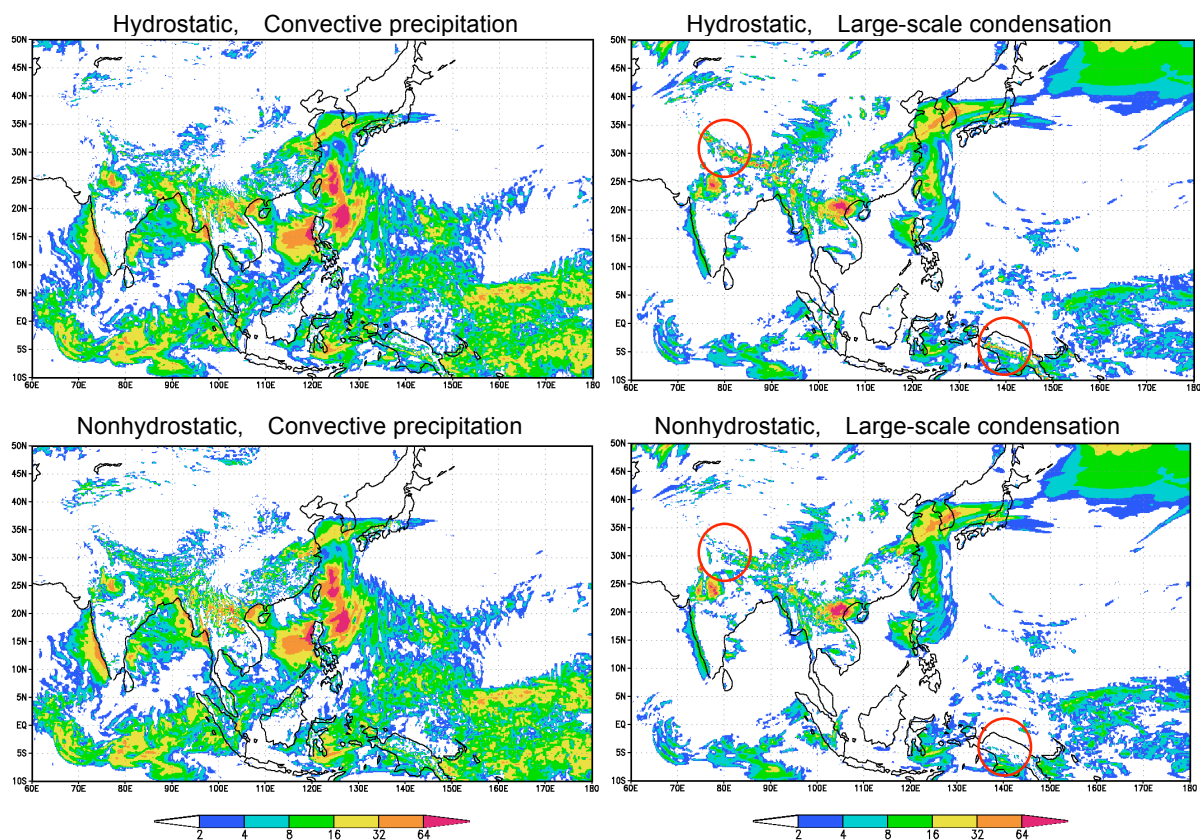

Fig. 1. 2-day mean convective and large-scale condensation precipitation of the hydrostatic and the nonhydrostatic models.

5. Reference

Bubnová R., G. Hello, P. Bénard, J.-F. Geleyn, 1995: Integration of the fully elastic equations cast in the hydrostatic pressure terrain-following coordinate in the framework of the ARPEGE/Aladin NWP system. *Mon. Wea. Rev.*, **123**, 515-535.

Bénard, P., J. Vivoda, J. Mašek, P. Smolíková, K. Yessad, Ch. Smith, R. Brožková and J.-F. Geleyn, 2010: Dynamical kernel of the Aladin-NH spectral limited-area model: Revised formulation and sensitivity experiments. *Q. J. R. Meteor. Soc.*, **136**, 155-169.

Cheong, H.-B., 2000: Application of Double Fourier Series to the Shallow-Water Equations on a Sphere. *J. Comput. Phy.*, **165**, 261-287.

Cheong, H.-B., I.-H. Kwon, T.-Y. Goo and M.-J. Lee, 2002: High-Order Harmonic Spectral Filter with the Double Fourier Series on a Sphere. *J. Comput. Phy.*, **177**, 313-335.

Miyamoto, K., 2006: Introduction of the Reduced Gaussian Grid into the Operational Global NWP model at JMA. *CAS/JSC WGNE Research Activities in Atmospheric and Ocean Modelling*, **36**, 6.9-6.10.

Miyamoto, K., 2009: Recent Improvements to the JMA Global NWP Model. *CAS/JSC WGNE Research Activities in Atmospheric and Ocean Modelling*, **39**, 6.9-6.10.

Wedi, N. P. and P. K. Smolarkiewicz, 2009: A framework for testing global non-hydrostatic models. *Q. J. R. Meteor. Soc.,* **135**, 469-484.

Yoshimura, H. and T. Matsumura, 2005: A two-time-level vertically-conservative semi-Lagrangian semi-implicit double Fourier series AGCM. *CAS/JSC WGNE Research Activities in Atmospheric and Ocean Modeling*, **35**, 3.25-3.26.

Yukimoto, S., et al., 2011: Meteorological Research Institute-Earth System Model Version 1 (MRI-ESM1) –Model Description–. *Technical Reports of the Meteorological Research Institute*, No. 64.